Accurate and non-invasive monitoring of biofilms in drinking water distribution systems through the analysis of quorum sensing-related mRNA in the effluent

Khuong Trinh[1)], Shota Konno[1)], Sangdo Yook[2)], Hyun-Suk Oh[3)], Chamteut Oh[1)]

1) Department of Environmental Engineering Sciences, University of Florida
2) Department of Chemical Engineering, University of Texas at Austin
3) Department of Environmental Engineering, Seoul National University of Science and Technology

- Khuong Trinh and Shota Konno contributed equally to this article.
- Corresponding authors: hyunsukoh@seoultech.ac.kr and chamteutoh@ufl.edu

15 **Graphical abstract**

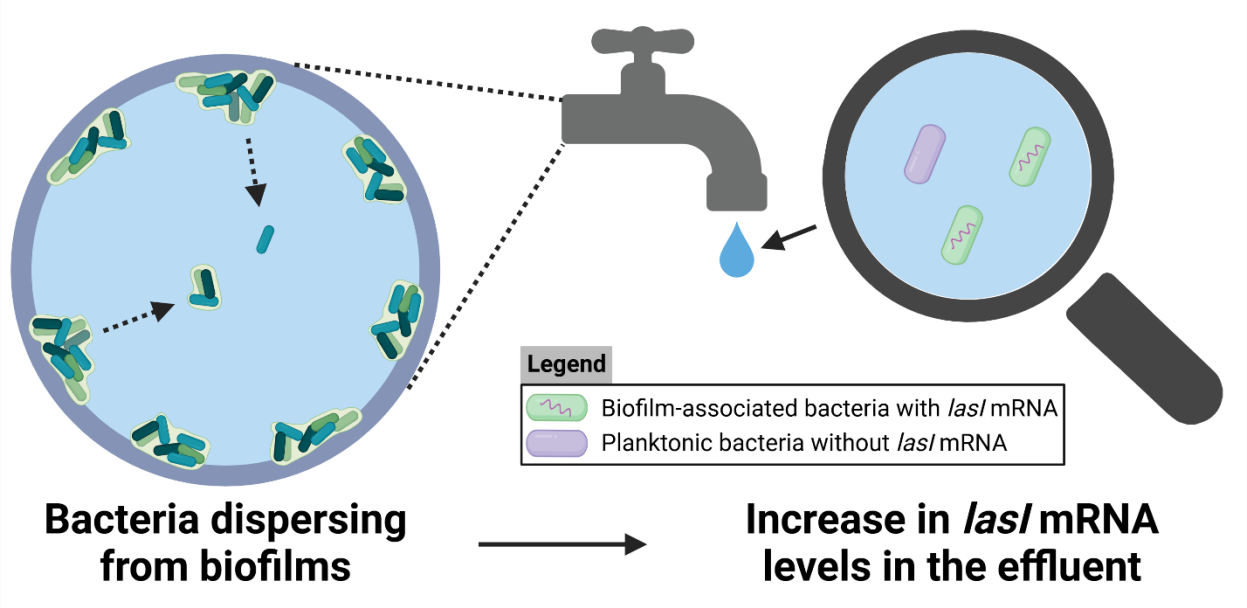

16

17

Abstract

Biofilm growth and dispersion in drinking water distribution systems (DWDS) pose risks to water quality and public health. Although monitoring biofilm formation in DWDS is essential for mitigating the risk of waterborne disease infections, current approaches that analyze the properties of the effluent cannot differentiate between planktonic and biofilm-associated bacteria. Quorum sensing (QS) systems are microbial communication mechanisms that regulate gene expression based on population density and are known to be more active in biofilm-associated bacteria than in planktonic bacteria. We hypothesize that bacteria dispersed from biofilms in DWDS influence QS-related mRNA levels detected in tap water effluent. Using *Pseudomonas aeruginosa* PAO1, a common bacterium found in DWDS, as a model organism, we examined the expression of the *lasI* gene, a key component of the *las* QS system, responsible for synthesizing QS signaling molecules. Specifically, the transcriptional activity of the *lasI* gene (i.e., RNA/DNA levels) in *P. aeruginosa* was systematically analyzed under various growth conditions. Our experiments confirmed that *P. aeruginosa* exhibits significantly higher *lasI* mRNA levels in biofilms compared to planktonic states. Additionally, we cultivated *P. aeruginosa* biofilms in flow channels and demonstrated that *lasI* mRNA levels in the effluent correlate with biofilm growth conditions within the flow channels. These findings indicate that biofilm growth in DWDS can be investigated non-invasively and accurately by analyzing *lasI* mRNA in the effluent. This rapid, non-invasive, and accurate biofilm monitoring approach has the potential to enable large-scale inspections and routine monitoring of biofilm growth within DWDS, ultimately improving public health.

Keywords

Biofilm monitoring; quorum sensing; drinking water; *Pseudomonas aeruginosa*; *lasI* gene

1. Introduction

Biofilms in drinking water distribution systems (DWDS) present significant challenges to water quality and safety. These microbial communities can adversely affect the aesthetic properties of water, leading to discoloration, as well as changes in odor and taste (Erdei-Tombor et al., 2024). More critically, biofilms act as reservoirs that protect potentially harmful microorganisms, including opportunistic pathogens such as *Legionella pneumophila*, *Mycobacterium avium*, and *Pseudomonas aeruginosa* (Waegenaar et al., 2024). Pathogens associated with biofilm may have enhanced resistance to disinfection, increased virulence potential, and potential for antibiotic resistance. Biofilms are also known to reduce residual disinfectant levels, causing unintended growth of pathogens (Fish et al., 2020; Xu et al., 2018). According to a Centers for Disease Control and Prevention (CDC) study conducted from 2015 to 2020, 28 states reported 214 drinking water-associated outbreaks, resulting in 2,140 cases of illness, 563 hospitalizations, and 88 deaths. Notably, 87% of these outbreaks were linked to biofilms in drinking water systems (Kunz et al., 2024). These biofilm-associated opportunistic pathogens cost the U.S. an estimated $2.39 billion annually (Healy et al., 2024). Additionally, 172 outbreaks (80%) were associated with water from public water systems, indicating that the source water itself was not the primary issue. This underscores the critical importance of effectively managing drinking water distribution systems to ensure public health protection. Early detection of biofilm formation is essential to enable timely intervention with minimal treatment (Erdei-Tombor et al., 2024).

Biofilm monitoring relies on both direct and indirect approaches. Direct approaches involve sampling biofilms by swabbing pipe surfaces or using coupons and microcosm reactors, followed by advanced analysis methods such as confocal laser scanning microscopy, molecular techniques (qPCR and 16S rDNA sequencing), direct cell count or biofilm activity assays

(Douterelo et al., 2016; Pick and Fish, 2024; Waller et al., 2018). While direct approaches provide detailed insights into biofilm composition, they are labor-intensive, location-specific, and fail to capture the dynamic nature of biofilm formation. In contrast, indirect approaches involve monitoring water quality parameters in effluent tap water, such as chlorine residuals, turbidity, microbial counts, and adenosine triphosphate (ATP) measurements(Addisie, 2022; Liu et al., 2016), which are indicative of the total bacterial count in the effluent. These methods are simpler, faster, more cost-effective, and applicable to a broader area of the DWDS compared to direct approaches. Additionally, they are non-invasive, allowing for routine monitoring across large distribution systems without disrupting the water supply. These advantages are essential for the early detection of biofilm formation and timely intervention (Liu et al., 2016). However, conventional indirect approaches lack specificity, often failing to differentiate biofilm-associated bacteria from planktonic bacteria, reducing their effectiveness for targeted management.

Given the limitations of current biofilm monitoring approaches, identifying an analyte unique to biofilm-associated bacteria could enable accurate detection of biofilms in the effluent. To this end, we focused on population density, as it is one of the significant differences between planktonic and biofilm-associated bacteria (Fish and Boxall, 2018; Mikkelsen et al., 2007). For example, Lopes et al., (2018) reported that population density of planktonic bacteria was in the range of 10^2–10^5 CFU/mL whereas that of biofilm-associated bacteria ranged between 10^5 and 10^7 CFU/cm² (i.e., 10^6 and 10^9 CFU/mL if the thickness is assumed to be 1 mm; (Neu et al., 2019)), showing several orders of magnitude higher cell density. Quorum sensing (QS) is a cell-to-cell communication system that enables bacteria to coordinate gene expression in response to population density (Rutherford and Bassler, 2012). QS plays a crucial role in biofilm formation by regulating bacterial attachment, biofilm maturation, and extracellular matrix production.

Specifically, bacteria secrete small signaling molecules, such as *N*-acyl-homoserine lactones (AHLs), which freely diffuse across cell membranes. As bacterial density increases, AHL concentrations accumulate, triggering the expression of QS-related genes. The *las* system is one of the well-characterized QS systems and plays a direct role in biofilm formation. Therefore, we hypothesize that *las* system mRNA in the effluent could serve as a specific biomarker for biofilm growth in DWDS.

Here, we introduce a novel approach for biofilm monitoring in DWDS. Our method is based on the analysis of effluent water quality, making it non-invasive. However, this approach is designed to improve accuracy by specifically detecting *las* mRNA from biofilm-associated bacteria in the effluent. In this study, we selected *P. aeruginosa* as a model bacterial species and systematically examined *las* mRNA expression in both planktonic and biofilm-associated bacteria. Our findings demonstrate that *las* mRNA signals in the effluent predominantly originate from biofilm-associated bacteria. Thus, our study suggests that detecting QS-related mRNA in the effluent provides a rapid, accurate, and non-invasive method for biofilm monitoring in DWDS.

2. Materials and methods

2.1. Experimental design

The model bacterial species used was *P. aeruginosa* PAO1, which is one of the best-studied environmental and opportunistic human pathogens for bacterial biofilm formation, was isolated from industrial wastewater sludge (Noori et al., 2022). We grew the bacteria in three different reactors: a small reactor, a large reactor, and a flow channel. Experiments with the small reactors were conducted to analyze all biofilm-associated bacteria on the reactor surface. For the small

reactor experiments, bacteria were first streaked onto LB agar plates and incubated at 37℃ overnight. We prepared the LB agar by suspending 40 g of LB agar powder (BP1425-500, Miller-Fisher BioReagents) in 1 liter of purified water (i.e., tryptone 10 g/L, yeast extract 5 g/L, sodium chlorine 10 g/L, and agar 15 g/L in the final solution). The mixture was sterilized at 121℃ for 15 minutes and cooled down to 40℃, and then distributed as 20 mL onto a 100 mm plate (430167, Corning). The following day, two fresh colonies were selected and diluted in 20 mL of LB broth in a 50 mL tube (339653, Thermo Fisher Scientific). The LB broth was prepared by adding 25 g of LB broth powder (BP9723-500, Miller-Fisher BioReagents) to 1 liter of purified water (i.e., tryptone 10 g/L, yeast extract 5 g/L, and sodium chlorine 10 g/L in the final solution), followed by sterilization at 121℃ for 15 minutes. The bacteria diluted in the LB broth was distributed as 0.5 mL in 1.5 mL tubes (3448PK, Thermo Fisher Scientific) and incubated at 37℃ without shaking for various incubation times ranging from 0 to 7 hours (**Figs 1 and 2**) or 0 to 4 days (**Fig. 4**). We assumed that planktonic bacteria existed in the culture media, while biofilm formed on the inner reactor wall. After incubation, the 0.5 mL of the culture media was gently sampled with a micropipette to minimize biofilm detachment. 140 µL sample was subjected to nucleic acid extraction, which was performed using the QIAamp Viral RNA Mini Kit (52906, QIAGEN) following the manufacturer's instruction (the final volume of elute was 60 µL). After sampling the 0.5 mL of culture media, the empty reactor was gently rinsed with molecular biology-grade water three times to minimize the presence of remaining planktonic bacteria. Then, 560 µL of lysing buffer was added to the reactor to lyse all biofilm-associated bacteria that had formed on the inner reactor wall during the incubation. We conducted a similar experiment with larger reactors to reduce biofilm-associated bacteria dispersed into planktonic bacteria analysis (**Fig. 3**). For this experiment, fresh colonies grown on agar plates were diluted

in 500 mL of LB broth in a 1 L glass bottle and incubated at 37°C without shaking for various incubation times ranging from 0 to 10 hours.

We conducted another experiment in which bacteria were grown in flow channels under flow conditions. Bacteria were diluted in 1 L of LB broth in a 1 L glass bottle. The culture media containing bacteria was fed using a peristaltic pump at a flow rate of 40 mL/min into fluorinated ethylene propylene (FEP) tubing (Tygon® Versilon™ SE-200, Saint-Gobain) with an inner diameter of 3.175 mm. The tubing was sterilized at 121°C for 15 minutes before the experimental setup. Bacteria grew in the culture media and on the inner tube wall under flow conditions at room temperature for various incubation times ranging from 18 to 147 hours. After incubation, a 10 cm section of the tubing was cut from the whole tubing. This section was then connected to a reservoir containing tap water, and the tap water was pumped through the tubing at a flow rate of 40 mL/min. We collected 2 L of effluent from the tubing, which was then filtered through a 0.22 µm filter to capture all bacteria in the effluent. After flowing 2 L of tap water, we cut the 10 cm tubing into small pieces so that they can be submerged in 1.68 mL (i.e., 560 µL × 3) of lysing buffer. This allowed for the extraction of nucleic acids from all biofilm-associated bacteria formed inside the tubing. We collected raw tap water samples that had not passed through the tube and analyzed their nucleic acid content as a negative control.

Additionally, we analyzed the tap water for pH, ORP, DO, and EC using a meter (HQ2200, HACH) with probes (PHC10101, MTC10101, LDO10101, and CDC40101, respectively, HACH) as well as free chlorine using a spectrophotometer (DR6000, HACH) following the manufacturer's protocol (80 Chlorine F & PP).

All experiments with the three types of reactors and sample preparations for molecular analyses, as described in the following section, were conducted in biosafety cabinets (1300

Series A2 from Thermo Scientific and Axiom C1 from Labconco), certified in accordance with ANSI/NSF 49.

2.2. Molecular analysis

Details about our (RT-)dPCR analysis were described following the Minimum Information for publication of Digital PCR Experiments (dMIQE guideline; **Table S1**). Nucleic acid extracts obtained from the nucleic acid extraction contained both DNA and RNA. The nucleic acid extracts were directly used for DNA analysis using a digital PCR (dPCR) system with the QIAcuity EvaGreen (EG) PCR Kit (250111, QIAGEN). Specifically, the dPCR mixture included 2 µL of nucleic acid extract, 0.6 µL of 8 µM forward primer, 0.6 µL of 8 µM reverse primer, 4 µL of 3x EvaGreen PCR Master Mix, and 4.8 µL of water. The dPCR mixture was loaded onto an 8.5k 24-well nanoplate with a fixed partition volume of 0.34 nL and analyzed using the QIAcuity One 5plex system (QIAGEN). The thermal cycling protocol consisted of one cycle at 95°C for 2 minutes, followed by 40 cycles of denaturation at 95°C for 15 seconds, annealing at 62°C for 15 seconds, and extension at 72°C for 15 seconds, with a final cooling step at 40°C for 5 minutes. The dPCR image was captured using the Green channel with an exposure duration of 200 ms and a gain of 6.

For RNA measurement, DNA was degraded from the nucleic acid extracts using the RNase-Free DNase Set (79254, QIAGEN). Specifically, 10 µL of Buffer RDD, 2.5 µL of DNase I stock solution, 47.5 µL of RNase-free water, and 40 µL of nucleic acid extract were combined in a 200 µL PCR tube. The tubes were then incubated at 25°C for 10 minutes, followed by heat treatment at 70°C for 15 minutes in a PCR thermocycler (Mastercycler x40, Eppendorf) to inactivate the DNase enzyme. For quality control of the DNase assay, we analyzed the nucleic

acid extracts that had contained DNA concentrations ranging from 5.1×10^4 to 4.6×10^5 gc/µL, for residual DNA after the assay. We confirmed that no residual DNA remained, indicating that RNA measurements originated solely from RNA in the samples (**Fig. S1**). The DNase-treated samples were subjected to RT-dPCR for RNA quantification using the QIAcuity OneStep Advanced EG Kit (250141, QIAGEN). The RT-dPCR mixture contained 2 µL of nucleic acid extract, 0.3 µL of 30 µM forward primer, 0.3 µL of 30 µM reverse primer, 3 µL of 4x OneStep Advanced EvaGreen PCR Master Mix, 0.12 µL of OneStep Advanced RT Mix, 1 µL of Q-solution, and 5.28 µL of RNase-free water. The RT-dPCR mixtures were loaded onto an 8.5k 24-well nanoplate and analyzed using the QIAcuity One 5plex system (QIAGEN). The thermal cycling protocol for RT-dPCR included incubation at 50°C for 40 minutes, followed by denaturation at 95°C for 2 minutes, then 40 cycles of denaturation at 95°C for 10 seconds, annealing and extension at 62°C for 30 seconds, and a final cooling step at 40°C for 5 minutes. The RT-dPCR image was captured using the Green channel with an exposure duration of 200 ms and a gain of 6.

All (RT-)dPCR analyses showed a distinct separation between positive and negative partitions (**Fig. S2**). The threshold for fluorescence intensity was set between 30 and 50 RFU to define positive and negative partitions. Samples for DNA and RNA analyses were diluted in molecular biology-grade water using multiple dilution factors if necessary, and the measurement with the number of positive partitions between 1,000 and 5,000 was selected to determine the final DNA or RNA concentration when available. The limit of detection was 2 gc/µL when the number of positive partitions was 1, at which the 95% confidence interval (CI) was 147.5%. The number of valid partitions was determined automatically with the information of the reference channel. Three biological replicates were conducted for each dataset, and one technical replicate

was analyzed per biological replicate. The confidence interval (CI) value for all analyses was less than 100%. All (RT-)dPCR analyses were conducted with molecular biology-grade water as a negative control. The highest number of positive partitions in the negative controls was less than 5, and the concentration of the negative control was subtracted from each measurement if a negative control exhibited positive partitions.

All samples collected from the experiments were immediately stored at −80°C. Once removed from the freezer, all assays, including nucleic acid extraction, the DNase assay, and (RT-)dPCR, were conducted immediately, and the entire process from sample thawing to loading into the dPCR system took approximately 3 hours. As a result, each sample underwent only one freeze-thaw cycle, minimizing the impact of nucleic acid degradation. Blank nucleic acid extractions were conducted each time a new experimental design was implemented, and all tested negative. We conducted an inhibition test for the nucleic acid extracts, and the impact of inhibitors in the extracts was negligible for (RT-)dPCR analysis (**Fig. S3A**). All (RT-)dPCR analyses were conducted by two researchers. We confirmed that the coefficient of variation in their RT-dPCR analysis was less than 5% in all cases, and their RT-dPCR results were not significantly different, indicating that the repeatability and reproducibility of RT-dPCR were acceptable (**Fig. S3B**).

Primer information for *lasI* and *lasB* genes is provided in **Table S2**. We confirmed through gel electrophoresis that the primer sets for *lasI* and *lasB* synthesized amplicons of the expected sizes and showed no primer dimer formation (**Fig. S4**). This finding indicates that these primers specifically amplified the target sequences, ensuring that positive (RT-)dPCR partitions did not result from non-specific amplification.

2.3. Statistical analysis

DNA and RNA concentrations between reaction times (**Figs. 1** and **2**) were compared using independent two-sample t-tests assuming unequal variances. Linear regression analysis was conducted to evaluate the goodness of fit using the coefficient of determination (R^2) or to assess the statistical significance of variables using the *p*-value (**Figs. 2, 3,** and **6**). All statistical analyses were conducted using Python 3.10.12 in Google Colab.

3. Results

3.1. Biofilm-associated bacteria transcribe significantly higher levels of *lasI* mRNA than planktonic bacteria

The model bacterium (*P. aeruginosa*) was grown in 1.5 mL-sized reactors. We analyzed both DNA and RNA obtained from the bulk solution and the reactor surface (**Fig. 1A**). **Fig. 1B** shows DNA obtained from the two compartments to represent planktonic and biofilm-associated bacterial counts, and the sum of the two represents the total bacterial count in the reactor. The red circle in **Fig. 1B** illustrates that the total bacterial count increased from hour 2 ($p<0.05$), with bacterial growth reaching saturation at hour 5. More specifically, while planktonic bacteria (green rectangle in **Fig. 1B**) began to increase at hour 2 ($p<0.05$), biofilm-associated bacteria (blue triangle in **Fig. 1B**) grew from hour 3 ($p<0.05$). This time discrepancy between the two types of bacteria is likely due to the time required for bacteria in the culture medium to attach and initiate biofilm formation. Additionally, although planktonic bacterial growth stopped at hour 3, biofilm-associated bacteria continued to increase until hour 7, when the experiment was completed. These results indicate that while planktonic bacteria were in the stationary phase, biofilm-associated bacteria remained in the exponential growth phase in this experiment.

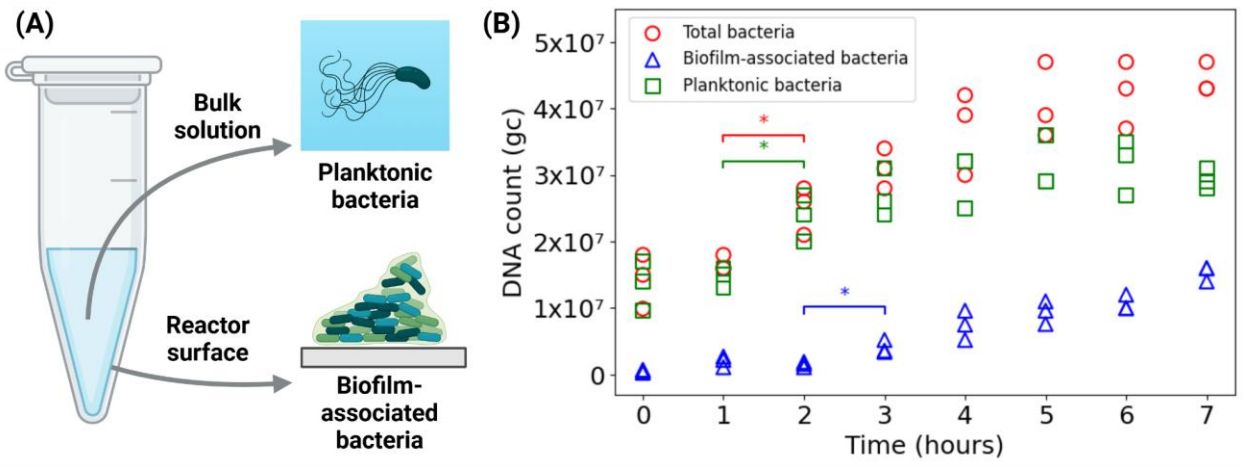

Fig. 1. (A) An illustration depicting two bacterial states in a reactor. (B) DNA counts obtained from both the bulk solution and the reactor surface indicate the total bacterial count (red circle), DNA counts only from the bulk solution represent planktonic bacteria (green rectangle), and DNA counts only from the reactor surface present biofilm-associated bacteria (blue triangle) over the incubation period. The target gene was *lasI*. Three biological replicates are presented for each incubation time. Statistical analyses were performed using a two-sample t-test (p<0.05, indicated by *).

We analyzed RNA/DNA levels of bacteria in each state (i.e., planktonic bacteria and biofilm-associated bacteria) to understand *lasI* mRNA transcriptional activity depending on bacterial modes of growth. The blue rectangle in **Fig. 2A** shows that the RNA/DNA levels of biofilm-associated bacteria significantly increased at hour 2 (p<0.05), prior to a significant increase in biofilm-associated bacterial count (red circle in **Fig. 2A**) at hour 3 (p<0.05). This result aligns with previous observations that the *lasI* gene is expressed before the biofilm biomass increases significantly (De Kievit et al., 2001; Duan and Surette, 2007). Additionally, the RNA/DNA levels increased as the biofilm-associated bacterial count increased throughout the experiment.

However, the RNA/DNA level of planktonic bacteria exhibited different trends from that of biofilm-associated bacteria (**Fig. 2B**). First, the increase in RNA/DNA levels of planktonic

bacteria did not precede an increase in planktonic bacterial count. Specifically, planktonic bacteria exhibited a significant increase in RNA/DNA levels at hour 2 (p<0.001), and bacterial count also increased at hour 2 (p<0.05). Second, the RNA/DNA levels of planktonic bacteria continued increasing between hours 2 and 7, during which the planktonic bacterial count did not change significantly (p>0.05). As a result, the coefficient of determination from the linear regression analysis for RNA/DNA levels and planktonic bacterial count (R^2 = 0.382 in **Fig. 2D**) was lower than that for biofilm-associated bacteria (R^2 = 0.648 in **Fig. 2C**).

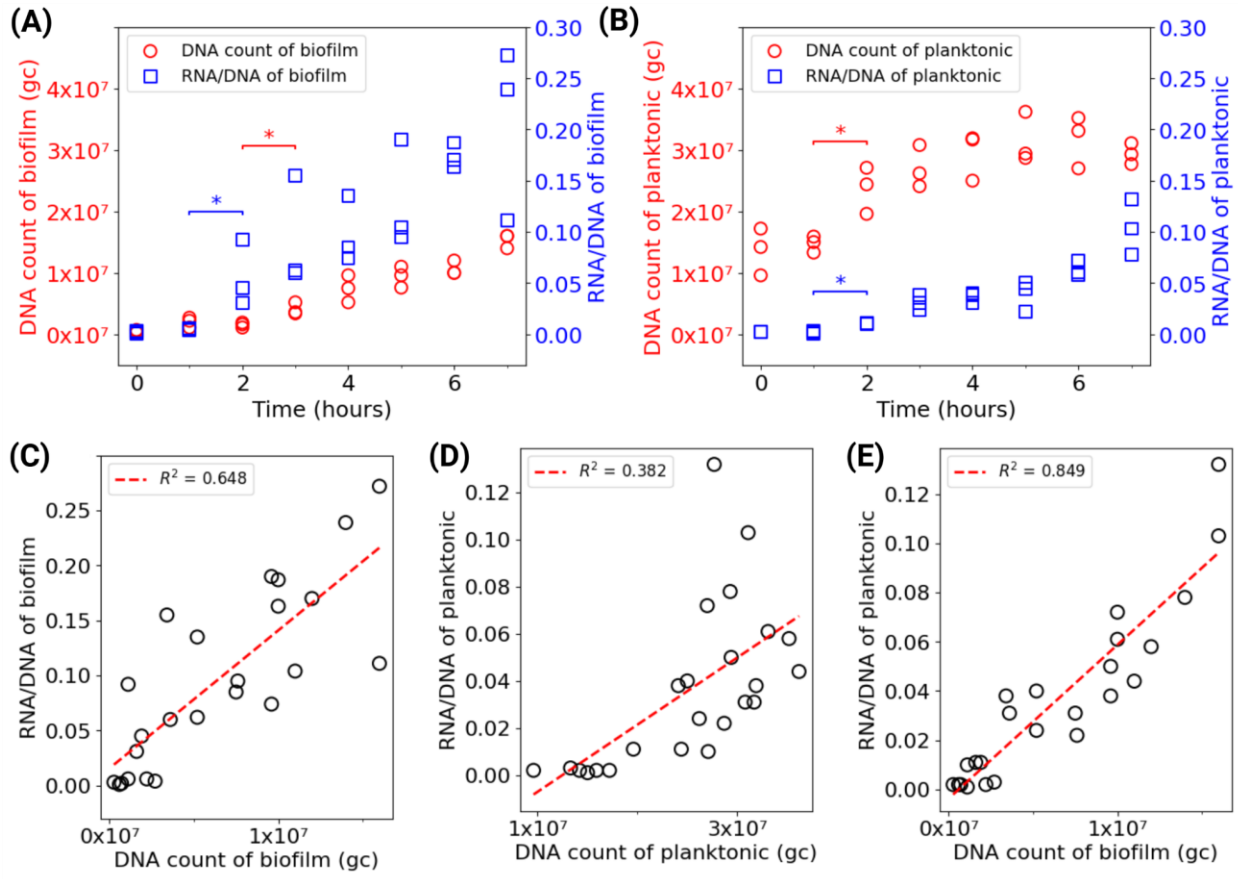

Fig. 2. Transcriptional activity (i.e., RNA/DNA) of *lasI* gene based on bacterial growth modes in small reactors. (A) and (B) show the DNA count and RNA/DNA level of biofilm-associated and planktonic bacteria over incubation time, respectively. A two-sample t-test was performed to confirm significant increases in DNA counts or RNA/DNA values between incubation times (p<0.05, indicated by *). (C), (D), and (E) illustrate the relationships between DNA count and

RNA/DNA level across different bacterial growth modes. Linear regression analyses were conducted (red dashed lines), and the corresponding R^2 values are presented.

RNA/DNA levels can increase when bacterial density exceeds a certain threshold (Miller and Bassler, 2001; Yan et al., 2021). We hypothesize that the increase in RNA/DNA levels of planktonic bacteria was not due to an increase in planktonic bacterial count but rather the dispersion of biofilm-associated bacteria into the bulk solution, based on the following observations. First, the increase in RNA/DNA levels of planktonic bacteria occurred simultaneously with that of biofilm-associated bacteria at hour 2. Second, the RNA/DNA levels of planktonic bacteria continued increasing until hour 7, during which the biofilm-associated bacterial count increased, whereas the planktonic bacterial count did not. Third, as a result, the RNA/DNA levels of planktonic bacteria showed a greater coefficient of determination with biofilm-associated bacterial count ($R^2 = 0.849$, **Fig. 2E**) than with planktonic bacteria count ($R^2 = 0.382$ in **Fig. 2D**).

To further support our hypothesis, we conducted another experiment with large reactors where the dispersion of biofilm-associated bacteria into the bulk solution was significantly reduced. The ratio of volume (cm^3) to surface area (cm^2) of the small reactor was 0.1 cm, while that of the large reactor was 1.8 cm. Therefore, we assumed that the fraction of bacteria dispersed from the biofilm into the bulk solution, relative to the planktonic bacteria in the bulk solution, was reduced in the large reactor. **Fig. 3** shows that the RNA/DNA levels of the bulk solution in large reactors did not increase significantly as planktonic bacterial concentration increased (linear regression; $p>0.05$). In contrast, the RNA/DNA levels of the bulk solution in small reactors increased rapidly. Notably, the planktonic bacterial concentrations in the large batch experiments encompassed those of the small batch experiments. This finding suggests that

the RNA/DNA levels of the bulk solution in the small batch experiments (**Fig. 1** and **2**) were less likely to have increased due to planktonic bacterial density exceeding a certain threshold but rather due to the dispersion of biofilm-associated bacteria into the bulk solution.

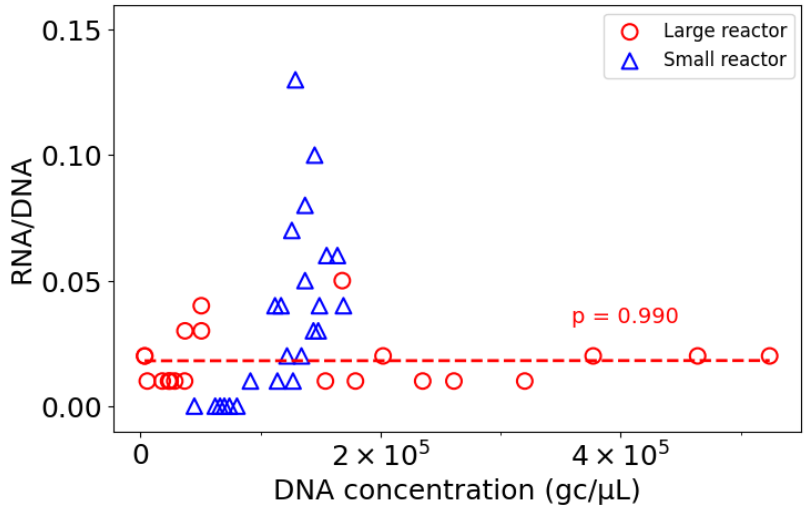

Fig. 3. Transcriptional activity (i.e., RNA/DNA) of the bulk solution in large (red circle) and small (blue triangle) reactors. The target gene was *lasI*. Linear regression analysis was conducted on the data from the large reactors.

We conducted another experiment with small reactors for a longer duration. **Fig. 4** shows that RNA/DNA levels peaked at hour 7 and plummeted at hour 24 when bacterial growth reached its peak. The diminishing *lasI* mRNA signal over time has also been reported in other studies (De Kievit et al., 2001). This finding suggests that *lasI* mRNA does not persist beyond a day once bacterial growth slows down. The degradation of *lasI* mRNA is likely due to sufficient translation of *lasI* enzymes, making high mRNA concentrations no longer necessary for bacterial activity.

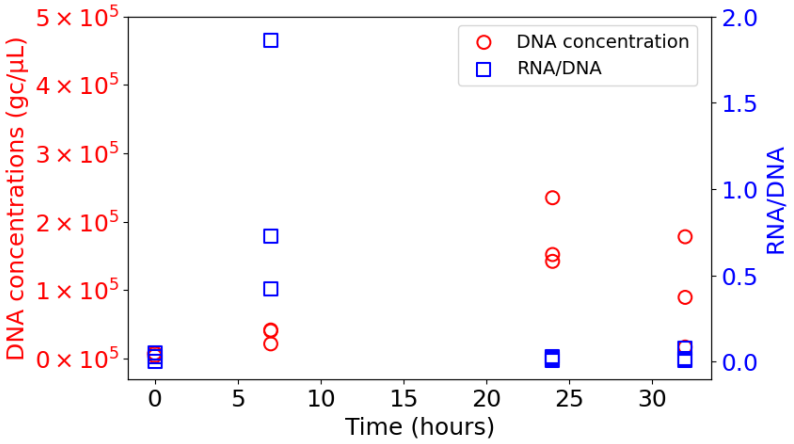

Fig. 4. Transcriptional activity (i.e., RNA/DNA) of bacteria in small reactors for prolonged incubation time until 32 hours. The target gene was *lasI*.

3.2. *lasI* mRNA in effluent originates from actively growing biofilm within the tubing through which the water flows

We grew bacteria in a tubing with a 3.175 mm diameter under flow conditions at 40 mL/min (**Fig. 5A**). Bacteria in the culture media grew exponentially until the end of the experiment (blue triangle in **Fig. 5B**). However, the biofilm-associated bacteria count (red circle in **Fig. 5B**) reached saturation much earlier, at approximately 44 hours. Unlike in the batch experiment, biofilm growth plateaued earlier, while planktonic bacteria continued to grow. This observation can be explained by an equilibrium between biofilm growth and the dispersion of biofilm-associated bacteria into the bulk solution due to the shear force of liquid flow.

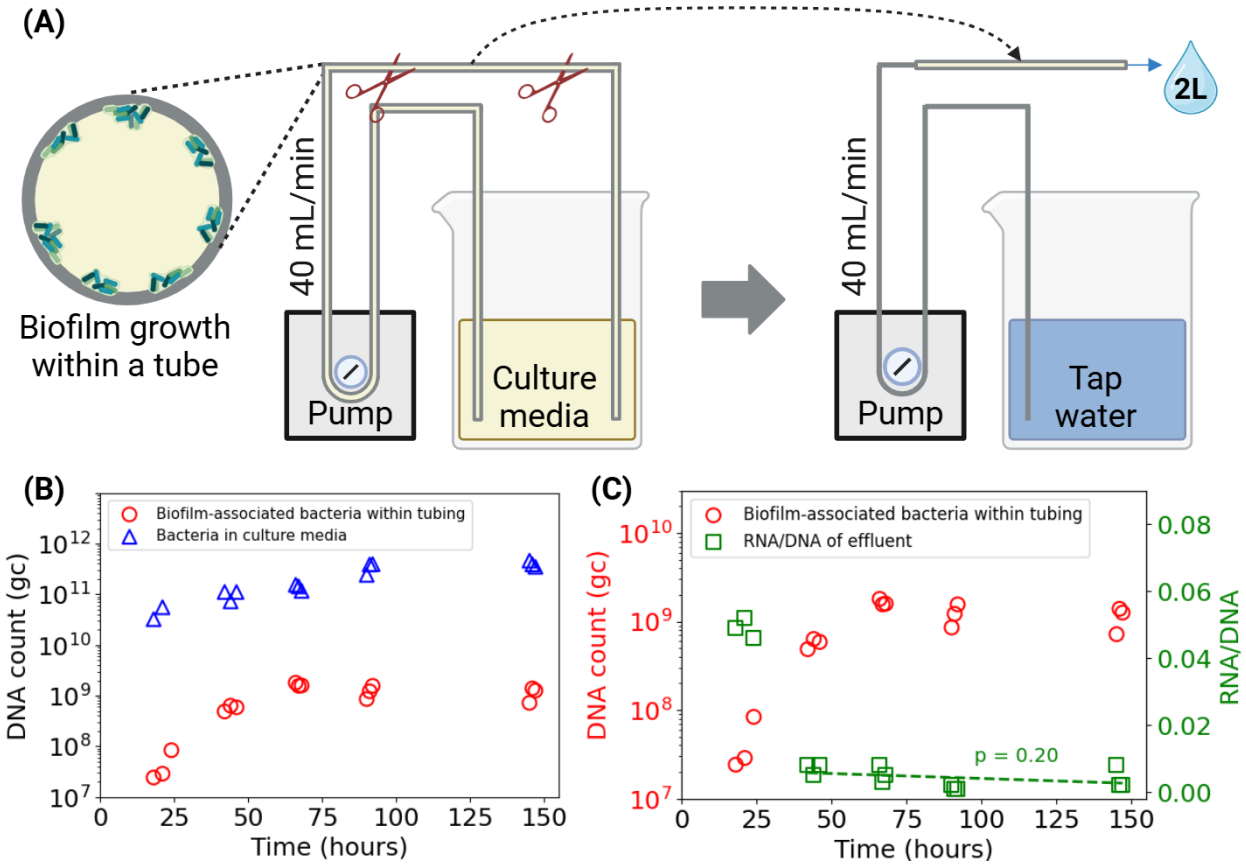

338

339 **Fig. 5.** (A) An experimental schematic depicting biofilm growth within tubing and its dispersion
340 into tap water under flow conditions. The biofilm developed inside the tubing under flow
341 conditions at 40 mL/min. After incubation for varying durations ranging from 18 to 147 hours, a
342 10 cm section of the tubing was cut, and 2 L of tap water was flowed through at 40 mL/min. (B)
343 Bacterial count in the bulk solution during biofilm growth (blue triangle). (C) RNA/DNA
344 concentration in 2 L of tap water passing through the 10 cm tubing (green rectangle). The
345 biofilm-associated bacterial count, obtained from the inner surface of the 10 cm tubing after
346 incubation, followed by the flow of 2 L of tap water, is presented as a red circle in (B) and (C).
347 The target gene was *lasI*.
348

349 We then cut the bacteria-grown tubing and flowed 2 L of tap water through it at 40
350 mL/min. The RNA/DNA level in the effluent (green rectangle) and the biofilm-associated
351 bacterial count within the tubing (red circle) are presented in **Fig. 5C**. When the biofilm was in
352 the exponential growth phase at approximately 20 hours, the RNA/DNA level in the effluent was
353 high, around 0.05. However, the RNA/DNA level dropped sharply to about 0.01 as the biofilm-
354 associated bacterial count reached saturation at approximately 44 hours. This value remained

355 constant as the biofilm-associated bacterial count stabilized at around 10^9 gc/tube (regression
356 analysis; p>0.05). Additionally, we verified that the RNA/DNA level in the effluent from the
357 tubing was proportional to that of biofilm-associated bacteria within the tube, with an R^2 value of
358 0.790 (**Fig. 6**). This finding suggests that the RNA/DNA level in the effluent originated from the
359 dispersion of biofilm-associated bacteria into the effluent.
360

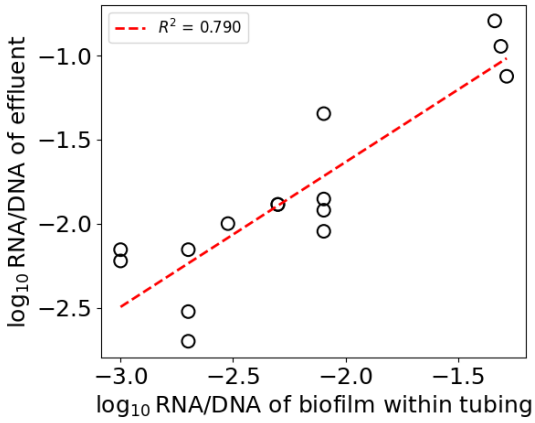

361

362 **Fig. 6**. Relationship between the RNA/DNA level of biofilm formed within the tubing and that
363 of the effluent, interpreted using linear regression analysis.
364

365 Note that we analyzed raw tap water that had not passed through the tubing as a control
366 experiment. The water properties, including temperature, pH, ORP, DO, EC, and free chlorine,
367 were 23.3±1.6°C, 8.6 ± 0.2, 235±42 mV, 434±16 μS/cm, 7.8±0.3 mg/L, and 0.09±0.06 mg/L,
368 respectively (n=7). These values align with typical tap water properties (Domoń et al., 2024; Oh
369 et al., 2024). We also analyzed the raw tap water for DNA and RNA using the same *lasI* primer
370 and (RT-)dPCR conditions. We found that the contribution of tap water to *lasI* DNA and RNA
371 signals in the effluent from the tubing experiment was below the detection limit. This finding
372 indicates that the RNA/DNA detected in the flow channel experiment originated from the
373 biofilm within the tubing.

4. Discussion

4.1. *lasI* mRNA is an appropriate biomarker for investigating biofilm formation

P. aeruginosa utilizes QS systems to regulate biofilm development, as well as the expression of various virulence factors, in a density-dependent manner (Sakuragi and Kolter, 2007). The *las* system is one of the well-studied QS systems in Gram-negative bacteria, including *P. aeruginosa*. Activation of genes related to the *las* system occurs in a hierarchical manner (Davies et al., 1998). First, the *lasI* gene synthesizes QS signals (e.g., 3-oxo-C12-HSL), which freely diffuse across the bacterial membrane and enable bacteria to sense their population density. More specifically, the *lasR* gene encodes the *lasR* protein, which forms a complex with the QS signals. This complex then induces the expression of virulence factors, including the *lasB* gene. The *lasB* gene encodes elastase, a proteolytic enzyme that degrades host extracellular matrix proteins such as elastin, collagen, and fibronectin (Galdino et al., 2019). This degradation process facilitates bacterial attachment to host surfaces and promotes biofilm maturation.

During the translation of *las*-related genes, the *lasI* gene is autoregulated by the *lasR*-QS signal complex, meaning that QS signals in the environment accelerate *lasI* gene expression. Furthermore, the *lasI* gene is activated at a lower QS signal concentration than other genes (Seed et al., 1995). We also conducted the small reactor experiments for the *lasB* gene, which is one of the *las*-related genes, but is not autoregulated and as sensitive to QS signals as *lasI* gene expression. As a result, the RNA/DNA level of *lasI* gene was much higher than that of *lasB* gene (**Fig. 2A** and **Fig. S5**). These findings suggest that *lasI* gene expression is rapid, highly sensitive to bacterial density, and upregulated in the early stages of biofilm formation. Therefore, *lasI* mRNA serves as a strong indicator of biofilm growth.

4.2. *lasI* mRNA in effluent indicates biofilm dispersion in drinking water distribution systems

The top layer of a biofilm is where biofilm-associated bacteria actively replicate as the biofilm grows from the surface upward (De Kievit et al., 2001). Additionally, planktonic bacteria in the surrounding fluid accumulate on the top layer of the biofilm. In other words, bacteria in the top layer are relatively newly introduced into the biofilm, either through bacterial reproduction within the biofilm or by the transfer of planktonic bacteria into the biofilm. Bacteria degrade *lasI* mRNA quickly, as confirmed in **Fig. 4** and previous studies (De Kievit et al., 2001), once a sufficient number of proteins has been translated. Thus, *lasI* mRNA of biofilm-associated bacteria primarily originates from bacteria in the top layer of the biofilm. Other studies also support that QS-related genes are more actively expressed in the top layer of the biofilm (Lidor et al., 2015). For example, Lenz et al., (2008) spatially visualized QS-related genes (*phzA1* and *aprA*) in biofilms and detected strong fluorescence signals derived from QS-related gene expression within 30 μm of the top layer, whereas fluorescence signals significantly weakened in biofilm regions deeper than 30 μm.

Our flow channel experiments were conducted when the biofilm, specifically the top layer, was in equilibrium between biofilm dispersion and biofilm growth. Therefore, it is reasonable to assume that the *lasI* mRNA detected in the effluent originates from bacteria dispersed from the biofilm. From a public health perspective, biofilm dispersion is important information because biofilm detachment into drinking water is directly related to the introduction of pathogens that have grown within the biofilm. For example, *L. pneumophila* can proliferate within biofilms in drinking water distribution systems and subsequently disperse back into the

drinking water, making it a major cause of waterborne disease infections in the U.S. (Huang et al., 2020a). Therefore, monitoring RNA/DNA levels in the effluent could serve as a novel approach to assessing the impact of biofilm on public health.

4.3. Environmental implications

Our systematic analysis of *lasI* gene transcriptional activity (i.e., RNA/DNA levels) supports our hypothesis that the RNA/DNA level in the effluent can represent biofilm growth in DWDS. This novel approach analyzes the effluent from DWDS, making the sampling process rapid and non-invasive. Furthermore, since *lasI* mRNA is a unique biomarker that distinguishes planktonic and biofilm-associated bacteria, it accurately indicates biofilm dispersion into the drinking water. This rapid, non-invasive, and accurate biofilm monitoring approach will enable large-scale inspections and routine monitoring of biofilm growth within DWDS, ultimately improving public health.

Our study has a few limitations. First, our experiment was conducted using a single model bacterial species (*P. aeruginosa*), whereas actual biofilms in DWDS contain complex microbial communities. Various AHL-based QS systems, such as *las*, *tra*, *rpa*, *rhl*, *cin*, and *esa*, have been reported in bacteria (Kylilis et al., 2018). In addition, other QS mechanisms, including AI-2, PQS, and DSF-based signaling, have also been closely linked to biofilm formation (Passos da Silva et al., 2017; Ryan et al., 2015). As a result, analyzing *asI* gene alone may not fully represent biofilm growth formed by diverse bacterial species. Therefore, future studies should explore representative QS systems that correlate highly with actual biofilm growth in DWDS. One possible approach is to conduct shotgun metagenomics and metatranscriptomics to better

understand the major QS systems present in the target drinking water and their transcriptional activities.

Second, we analyzed bacteria in the bulk solution and on the reactor surface to represent planktonic and biofilm-associated bacteria, respectively. Given that the reactor surface was the primary site for biofilm growth, this approach was reasonable. Although our experimental results strongly suggest that the bulk solution contained bacteria dispersed from the biofilm, we did not obtain direct evidence that the RNA/DNA detected in the effluent originated from biofilm-associated bacteria. Thus, future studies should design alternative experimental setups to directly examine the dispersion of biofilm-associated bacteria. One possible approach is to engineer bacteria to fluoresce upon QS-related gene expression and grow them in a microfluidic system. Real-time fluorescence monitoring using microscopy would allow visual tracking of mRNA-producing bacteria in drinking water.

Third, our experimental findings suggest that mRNA levels in the effluent are proportional to bacterial dispersion from the biofilm. Biofilm dispersion is influenced by various factors, including flow rate, which is directly related to the shear force applied to biofilm detachment, and water chemistry, which affects biofilm physical properties such as porosity and elasticity (Clark et al., 2024; Huang et al., 2023a, 2023b, 2020b; Shi et al., 2022). Thus, future studies should investigate RNA/DNA levels in the effluent from DWDS under diverse environmental conditions to better understand these relationships.

5. Conclusions

This study presents a rapid, non-invasive, and accurate approach for monitoring biofilm growth in DWDS by analyzing the transcriptional activity of QS-related genes (i.e., RNA/DNA levels)

in the effluent. Our findings demonstrate that *lasI*-like QS synthase mRNA can serve as a reliable biomarker specifically associated with biofilm growth and its dispersion from DWDS. Given the critical role of biofilms in harboring opportunistic pathogens, implementing this mRNA-based biofilm monitoring strategy could significantly improve public health by providing real-time insights into biofilm dynamics and enabling large-scale DWDS monitoring without disrupting the water supply.

Acknowledgment

This study was funded through a start-up package for Dr. Chamteut Oh from the Department of Environmental Engineering Sciences at the University of Florida. This work was also supported by the National Research Foundation of Korea (NRF) grant funded by the Korean Government (MSIT) (RS-2024-00352287).

References

Addisie, M.B., 2022. Evaluating Drinking Water Quality Using Water Quality Parameters and Esthetic Attributes. Air, Soil and Water Research 15. https://doi.org/10.1177/11786221221075005/ASSET/IMAGES/LARGE/10.1177_11786221221075005-FIG2.JPEG

Clark, G.G., Geisler, D., Coey, E.J., Pollitz, L.J., Zaki, F.R., Huang, C., Boppart, S.A., Nguyen, T.H., 2024. Influence of phosphate on bacterial release from activated carbon point-of-use filters and on biofilm characteristics. Science of The Total Environment 914, 169932. https://doi.org/10.1016/J.SCITOTENV.2024.169932

Davies, D.G., Parsek, M.R., Pearson, J.P., Iglewski, B.H., Costerton, J.W., Greenberg, E.P., 1998. The involvement of cell-to-cell signals in the development of a bacterial biofilm. Science (1979) 280, 295–298. https://doi.org/10.1126/SCIENCE.280.5361.295/ASSET/FB9F64D1-C794-46CC-BAF6-518822A5C195/ASSETS/GRAPHIC/SE1486404003.JPEG

De Kievit, T.R., Gillis, R., Marx, S., Brown, C., Iglewski, B.H., 2001. Quorum-Sensing Genes in Pseudomonas aeruginosa Biofilms: Their Role and Expression Patterns. Appl Environ Microbiol 67, 1865. https://doi.org/10.1128/AEM.67.4.1865-1873.2001

Domoń, A., Kowalska, B., Papciak, D., Wojtaś, E., Kamińska, I., 2024. Safety of Tap Water in Terms of Changes in Physical, Chemical, and Biological Stability. Water 2024, Vol. 16, Page 1221 16, 1221. https://doi.org/10.3390/W16091221

Douterelo, I., Jackson, M., Solomon, C., Boxall, J., 2016. Microbial analysis of in situ biofilm formation in drinking water distribution systems: implications for monitoring and control of drinking water quality. Appl Microbiol Biotechnol 100, 3301–3311. https://doi.org/10.1007/S00253-015-7155-3/FIGURES/5

Duan, K., Surette, M.G., 2007. Environmental regulation of Pseudomonas aeruginosa PAO1 las and Rhl quorum-sensing systems. J Bacteriol 189, 4827–4836. https://doi.org/10.1128/JB.00043-07/ASSET/21B18332-8228-4879-9F55-C5B09CB7E5DB/ASSETS/GRAPHIC/ZJB0130768760007.JPEG

Erdei-Tombor, P., Kiskó, G., Taczman-Brückner, A., 2024. Biofilm Formation in Water Distribution Systems. Processes 2024, Vol. 12, Page 280 12, 280. https://doi.org/10.3390/PR12020280

Fish, K.E., Boxall, J.B., 2018. Biofilm microbiome (re)growth dynamics in drinking water distribution systems are impacted by chlorine concentration. Front Microbiol 9, 2519. https://doi.org/10.3389/FMICB.2018.02519/FULL

Fish, K.E., Reeves-McLaren, N., Husband, S., Boxall, J., 2020. Uncharted waters: the unintended impacts of residual chlorine on water quality and biofilms. npj Biofilms and Microbiomes 2020 6:1 6, 1–12. https://doi.org/10.1038/s41522-020-00144-w

Galdino, A.C.M., Viganor, L., De Castro, A.A., Da Cunha, E.F.F., Mello, T.P., Mattos, L.M., Pereira, M.D., Hunt, M.C., O'Shaughnessy, M., Howe, O., Devereux, M., McCann, M., Ramalho, T.C., Branquinha, M.H., Santos, A.L.S., 2019. Disarming Pseudomonas aeruginosa virulence by the inhibitory action of 1,10-phenanthroline-5,6-dione-based compounds: Elastase B (lasB) as a chemotherapeutic target. Front Microbiol 10, 1701. https://doi.org/10.3389/FMICB.2019.01701/FULL

Healy, H.G., Ehde, A., Bartholow, A., Kantor, R.S., Nelson, K.L., 2024. Responses of drinking water bulk and biofilm microbiota to elevated water age in bench-scale simulated distribution systems. npj Biofilms and Microbiomes 2024 10:1 10, 1–18. https://doi.org/10.1038/s41522-023-00473-6

Huang, C., Clark, G.G., Zaki, F.R., Won, J., Ning, R., Boppart, S.A., Elbanna, A.E., Nguyen, T.H., 2023a. Effects of phosphate and silicate on stiffness and viscoelasticity of mature biofilms developed with simulated drinking water. Biofouling 39, 36–46. https://doi.org/10.1080/08927014.2023.2177538

Huang, C., Ginn, T.R., Clark, G.G., Zaki, F.R., Won, J., Boppart, S.A., Nguyen, T.H., 2023b. Phosphate-Based Corrosion Inhibition in Drinking Water Systems and Effects on Disinfectant Decay and Biofilm Growth. Environ Eng Sci 40, 634–644. https://doi.org/10.1089/EES.2023.0065/ASSET/IMAGES/EES.2023.0065_FIGURE5.JPG

Huang, C., Shen, Y., Smith, R.L., Dong, S., Nguyen, T.H., 2020a. Effect of disinfectant residuals on infection risks from Legionella pneumophila released by biofilms grown under simulated premise plumbing conditions. Environ Int 137, 105561. https://doi.org/10.1016/J.ENVINT.2020.105561

Huang, C., Sun, P.P., Won, J., Wang, Y., Boppart, S.A., Nguyen, T.H., 2020b. Effect of Nonphosphorus Corrosion Inhibitors on Biofilm Pore Structure and Mechanical Properties. Environ Sci Technol 54, 14716–14724. https://doi.org/10.1021/ACS.EST.0C04645/ASSET/IMAGES/LARGE/ES0C04645_0007.JPEG

Kunz, J.M., Lawinger, H., Miko, S., Gerdes, M., Thuneibat, M., Hannapel, E., Roberts, V.A., 2024. Surveillance of Waterborne Disease Outbreaks Associated with Drinking Water — United States, 2015–2020. MMWR. Surveillance Summaries 73, 1–23. https://doi.org/10.15585/MMWR.SS7301A1

Kylilis, N., Tuza, Z.A., Stan, G.B., Polizzi, K.M., 2018. Tools for engineering coordinated system behaviour in synthetic microbial consortia. Nature Communications 2018 9:1 9, 1–9. https://doi.org/10.1038/s41467-018-05046-2

Lenz, A.P., Williamson, K.S., Pitts, B., Stewart, P.S., Franklin, M.J., 2008. Localized gene expression in Pseudomonas aeruginosa biofilms. Appl Environ Microbiol 74, 4463–4471. https://doi.org/10.1128/AEM.00710-08/ASSET/E032A300-8170-4FBB-B0D2-4FBFDAF1D84D/ASSETS/GRAPHIC/ZAM0140890120005.JPEG

Lidor, O., Al-Quntar, A., Pesci, E.C., Steinberg, D., 2015. Mechanistic analysis of a synthetic inhibitor of the Pseudomonas aeruginosa LasI quorum-sensing signal synthase. Scientific Reports 2015 5:1 5, 1–13. https://doi.org/10.1038/srep16569

Liu, S., Gunawan, C., Barraud, N., Rice, S.A., Harry, E.J., Amal, R., 2016. Understanding, monitoring, and controlling biofilm growth in drinking water distribution systems. Environ Sci Technol 50, 8954–8976. https://doi.org/10.1021/ACS.EST.6B00835/ASSET/IMAGES/LARGE/ES-2016-00835V_0004.JPEG

Lopes, S.P., Azevedo, N.F., Pereira, M.O., 2018. Quantitative assessment of individual populations within polymicrobial biofilms. Scientific Reports 2018 8:1 8, 1–13. https://doi.org/10.1038/s41598-018-27497-9

Mikkelsen, H., Duck, Z., Lilley, K.S., Welch, M., 2007. Interrelationships between Colonies, Biofilms, and Planktonic Cells of Pseudomonas aeruginosa. J Bacteriol 189, 2411. https://doi.org/10.1128/JB.01687-06

Miller, M.B., Bassler, B.L., 2001. Quorum sensing in bacteria. Annu Rev Microbiol 55, 165–199. https://doi.org/10.1146/ANNUREV.MICRO.55.1.165

Neu, L., Proctor, C.R., Walser, J.C., Hammes, F., 2019. Small-scale heterogeneity in drinking water biofilms. Front Microbiol 10, 2446. https://doi.org/10.3389/FMICB.2019.02446/FULL

Noori, A., Kim, H., Kim, M.H., Kim, K., Lee, K., Oh, H.S., 2022. Quorum quenching bacteria isolated from industrial wastewater sludge to control membrane biofouling. Bioresour Technol 352, 127077. https://doi.org/10.1016/J.BIORTECH.2022.127077

Oh, C., Zheng, G., Samineni, L., Kumar, M., Nguyen, T.H., 2024. Effective Removal of Enteric Viruses by Moringa oleifera Seed Extract Functionalized Cotton Filter. ACS ES and T Water 4, 3320–3331. https://doi.org/10.1021/ACSESTWATER.4C00194/ASSET/IMAGES/LARGE/EW4C00194_0004.JPEG

Passos da Silva, D., Schofield, M.C., Parsek, M.R., Tseng, B.S., 2017. An Update on the Sociomicrobiology of Quorum Sensing in Gram-Negative Biofilm Development. Pathogens 2017, Vol. 6, Page 51 6, 51. https://doi.org/10.3390/PATHOGENS6040051

Pick, F.C., Fish, K.E., 2024. Emerging investigator series: optimisation of drinking water biofilm cell detachment and sample homogenisation methods for rapid quantification via flow cytometry. Environ Sci (Camb) 10, 797–813. https://doi.org/10.1039/D3EW00553D

Rutherford, S.T., Bassler, B.L., 2012. Bacterial Quorum Sensing: Its Role in Virulence and Possibilities for Its Control. Cold Spring Harb Perspect Med 2, a012427. https://doi.org/10.1101/CSHPERSPECT.A012427

Ryan, R.P., An, S. qi, Allan, J.H., McCarthy, Y., Dow, J.M., 2015. The DSF Family of Cell–Cell Signals: An Expanding Class of Bacterial Virulence Regulators. PLoS Pathog 11, e1004986. https://doi.org/10.1371/JOURNAL.PPAT.1004986

Sakuragi, Y., Kolter, R., 2007. Quorum-sensing regulation of the biofilm matrix genes (pel) of Pseudomonas aeruginosa. J Bacteriol 189, 5383–5386. https://doi.org/10.1128/JB.00137-07/ASSET/D1B9C0E1-F3FD-430F-AEEF-165FEF3A892B/ASSETS/GRAPHIC/ZJB0140769430003.JPEG

Seed, P.C., Passador, L., Iglewski, B.H., 1995. Activation of the Pseudomonas aeruginosa lasI gene by LasR and the Pseudomonas autoinducer PAI: an autoinduction regulatory hierarchy. J Bacteriol 177, 654–659. https://doi.org/10.1128/JB.177.3.654-659.1995

Shi, X., Clark, G.G., Huang, C., Nguyen, T.H., Yuan, B., 2022. Chlorine decay and disinfection by-products formation during chlorination of biofilms formed with simulated drinking water containing corrosion inhibitors. Science of The Total Environment 815, 152763. https://doi.org/10.1016/J.SCITOTENV.2021.152763

Waegenaar, F., García-Timermans, C., Van Landuyt, J., De Gusseme, B., Boon, N., 2024. Impact of operational conditions on drinking water biofilm dynamics and coliform invasion potential. Appl Environ Microbiol 90, e00042-24. https://doi.org/10.1128/AEM.00042-24

Waller, S.A., Packman, A.I., Hausner, M., 2018. Comparison of biofilm cell quantification methods for drinking water distribution systems. J Microbiol Methods 144, 8–21. https://doi.org/10.1016/J.MIMET.2017.10.013

609 Xu, J., Huang, C., Shi, X., Dong, S., Yuan, B., Nguyen, T.H., 2018. Role of drinking water
610 biofilms on residual chlorine decay and trihalomethane formation: An experimental and
611 modeling study. Science of The Total Environment 642, 516–525.
612 https://doi.org/10.1016/J.SCITOTENV.2018.05.363
613 Yan, C., Li, X., Zhang, G., Zhu, Y., Bi, J., Hao, H., Hou, H., 2021. Quorum Sensing-Mediated
614 and Growth Phase-Dependent Regulation of Metabolic Pathways in Hafnia alvei H4. Front
615 Microbiol 12, 567942. https://doi.org/10.3389/FMICB.2021.567942/BIBTEX
616